Electronic structure and binding energies of hydrogen-decorated vacancies in Ni

H. Zheng,* B. K. Rao, S. N. Khanna, and P. Jena
Physics Department, Virginia Commonwealth University, Richmond, Virginia 23284-2000
(Received 20 May 1996; revised manuscript received 18 October 1996)

The electronic structure, binding energies, and magnetic properties of Ni-containing vacancies and vacancy-hydrogen complexes have been studied using a first-principles all-electron self-consistent embedded-cluster model based on local-spin-density-functional theory. The results describe the properties of perfect ferromagnetic Ni metal correctly. The calculated local-spin magnetic moment at the nearest-neighbor site of the monovacancy is found to be 30% larger than the bulk value. This magnetic moment, however, is reduced significantly as hydrogen occupies the vacancy center. Calculations of binding energies of six hydrogen atoms moving along the octahedral directions from the vacancy center reveal that the magnetic moments at the nearest-neighbor Ni site continually decrease, eventually coupling antiferromagnetically to the bulk moment. This occurs when hydrogen atoms are displaced from the vacancy center by a distance of $a_0/2$, where a_0 is the lattice constant. This is analogous to the antiferromagnetic coupling in NiO. The trapping of a six-hydrogen-atom complex inside a vacancy is found to be energetically favorable. The results are compared with a recent experiment where copious vacancy formation under high hydrogen pressure and temperature was observed. [S0163-1829(97)05807-4]

I. INTRODUCTION

The interaction of hydrogen with metals has been a topic of interest for more than a century not only because hydrogen is the smallest impurity atom, but also because metal-hydrogen systems are technologically important. Trapping of hydrogen at lattice defects has important consequences for understanding hydrogen embrittlement. Vacancies are one of the most basic types of point defects. A typical vacancy concentration at the melting point of a metal is about 10^{-3}. It has also been known that vacancies trap hydrogen and the preferential site for hydrogen is off the vacancy center. It was not until a couple of years ago that the influence of hydrogen on vacancy formation was demonstrated.

Fukai and Okuma[1] carried out an *in situ* x-ray-diffraction study of Ni and Pd under high pressure ($\sim$5 GPa) and high temperature ($\sim$800 °C). They observed an anomalous lattice contraction amounting to $\sim$0.5 Å^3 per metal atom in the hydride phase. This contraction remained even after hydrogen was removed by heating the sample to 400 °C, but was annealed out at 800 °C. They attributed this lattice contraction to the copious amount of vacancy formation ($\sim$20%) induced by the presence of hydrogen.

The quantitative understanding of vacancy trapping of hydrogen from theoretical calculations is a difficult problem. The presence of defects destroys crystalline order, making conventional band-structure calculations difficult. To circumvent the difficulty associated with the loss of periodicity, a supercell can be constructed that contains the defect and a number of surrounding host atoms. The supercells can then be repeated periodically. Electronic band-structure techniques for this superlattice can be used to calculate the energetics of the system. When hydrogen atoms are trapped by a vacancy, the calculations can get more complicated as one does not *a priori* know if hydrogen atoms would occupy the vacancy center or be displaced. Multiple trapping of hydrogen atoms by a single vacancy is even a harder problem to study from first principles. The relaxation of the host lattice around the vacancy-hydrogen complex as well as the zero-point vibration of the hydrogen are almost impossible to treat in a first-principles theory.

A semiquantitative understanding of hydrogen trapping by vacancies has been made possible by using effective-medium theories. The embedding energy of a hydrogen atom at any particular site is approximated by calculating the ambient electron density at that site and assuming that the response to hydrogen is as if it is embedded in a homogeneous electron gas of that density. Higher-order corrections can be made, but the model remains, in principle, semiquantitative. In addition, this model cannot provide any information on the electronic structure or magnetism of the imperfect system. Nevertheless, the effective-medium theory has correctly revealed that the hydrogen atom tends to remain at an off-center site in the metal vacancy.[2]

A method that has been successfully applied to study the electronic structure as well as energetics of defects in metals and is intermediate between the supercell and effective-medium approach in terms of complexity is based on the molecular-cluster model. Here the defected system is approximated by a cluster of host atoms surrounding the defect site. The electronic structure and total energies can be calculated self-consistently by using the standard molecular-orbital theory based on the linear combination of atomic orbitals method. Since the model is based on real-space formalism, the loss of periodicity due to the defect does not, in principle, pose any real problem, although use of symmetry relations can substantially lower computational time. In addition, computational considerations usually limit the cluster size to only a few atoms, thus raising the nagging question of whether the cluster size is large enough.

Recently, attempts have been made to address this shortcoming in the cluster model. This is done by embedding the cluster in a larger matrix of host atoms and taking into account the coupling between the central cluster with the em-

bedding medium self-consistently. This method, while minimizing the boundary effects, can also treat the electronic and magnetic interactions properly. The self-consistent cluster-embedding (SCCE) method is a first-principles method that has been successfully applied to transition-metal monoxides NiO and CoO,[3–5] but has not been used for metals. For nonperiodic systems containing impurities and surface states, the SCCE method should be more suitable than other methods because of the localized property of its solutions.

In this paper, we have used the SCCE method to calculate the electronic structure, magnetic properties, and binding energies of pure Ni metal, monovacanies in Ni, and vacancies decorated with one and six hydrogen atoms. In Sec. II we outline briefly the theoretical method. The results are presented in Sec. III and summarized in Sec. IV.

II. SELF-CONSISTENT CLUSTER-EMBEDDING METHOD

Although this method has been described in detail elsewhere,[3] we provide a brief overview of our procedure for completeness. In this model, we divide the system into two regions. The central core region (region I) contains the defect and a small number of host atoms $M_{\rm I}$ occupying sites they would normally occupy in the lattice. This cluster is embedded in a larger cluster of outer atoms $M_{\rm II}$ (region II) that simulates the bulk environment. The total number of atoms considered in our calculation is $M=M_{\rm I}+M_{\rm II}$.

The starting point of our calculation is the density-functional theory of Hohenberg, Kohn, and Sham[6,7] where the ground-state energy of N interacting electrons in a field of M fixed nuclei is given by

$$E_G[\rho]=T[\rho]+E_{\rm xc}[\rho]+\int\int\frac{\rho(\mathbf{r})\rho(\mathbf{r}')}{|\mathbf{r}-\mathbf{r}'|}\,d\mathbf{r}\,d\mathbf{r}'-2\sum_{i=1}^{M}\int\frac{\rho(\mathbf{r})Z_i}{|\mathbf{r}-\mathbf{R}_i|}\,d\mathbf{r}+\sum_{\substack{i,j\\ i\neq j}}^{M}\frac{Z_iZ_j}{|\mathbf{R}_i-\mathbf{R}_j|}. \quad (1)$$

Here $T[\rho]$ is the total kinetic energy of N noninteracting electrons. $E_{\rm xc}[\rho]$ is the exchange-correlation energy[8,9] of the system. Atomic units are used throughout this paper ($e^2=2$, $\hbar=1$, and $2m_e=1$). The charge density $\rho(\mathbf{r})$ is the sum of spin-up ($\uparrow$) and -down ($\downarrow$) densities, namely,

$$\rho(\mathbf{r})=\rho^{\uparrow}(\mathbf{r})+\rho^{\downarrow}(\mathbf{r}). \quad (2)$$

The kinetic energy T is evaluated exactly while the exchange-correlation term $E_{\rm xc}$ is calculated by the local-spin-density approximation. Let $\rho_{\rm I}$ and $\rho_{\rm II}$ represent the total electron charge density in regions I and II, respectively. The total electron density of the embedded medium is then

$$\rho(\mathbf{r})=\rho_{\rm I}(\mathbf{r})+\rho_{\rm II}(\mathbf{r}). \quad (3)$$

Assume that $\rho_{\rm II}(\mathbf{r})$ is already known and fixed. $\rho_{\rm I}(\mathbf{r})$ can be written as

$$\rho_{\rm I}(\mathbf{r})=\rho_{\rm I}^{\uparrow}(\mathbf{r})+\rho_{\rm I}^{\downarrow}(\mathbf{r})=\sum_{\text{occupied }n\rm I}|\phi_{n\rm I}^{\uparrow}(\mathbf{r})|^2+\sum_{\text{occupied }n\rm I}|\phi_{n\rm I}^{\downarrow}(\mathbf{r})|^2. \quad (4)$$

The $\phi_n^{\sigma}(\mathbf{r})$'s are composed of linear combination of atomic orbitals. By varying $\phi_n^{\sigma}(\mathbf{r})$ under the constraint that $\delta\int\rho_{\rm I}(\mathbf{r})d\mathbf{r}=0$, one gets the traditional Kohn-Sham equations

$$\left(-\nabla^2+2\int\frac{\rho_{\rm I}(\mathbf{r}')+\rho_{\rm II}(\mathbf{r}')}{|\mathbf{r}-\mathbf{r}'|}\,d\mathbf{r}'-2\sum_{i=1}^{M}\frac{Z_i}{|\mathbf{r}-\mathbf{R}_i|}+V_{\rm xc}^{\sigma}(\mathbf{r})\right)\phi_n^{\sigma}(\mathbf{r})=\lambda_n^{\sigma}\phi_n^{\sigma}(\mathbf{r}). \quad (5)$$

Note that, unlike in the energy band theory, the one-electron wave functions $\phi_n^{\sigma}(r)$ in Eq. (5) are localized. They represent only a small part of the electron system: the cluster electrons in region I. In addition, the $\rho_{\rm I}(\mathbf{r})$, constructed from the solutions of Eq. (5), makes the total energy minimum with respect to a fixed $\rho_{\rm II}(\mathbf{r})$.

In order to prevent the electrons of the central cluster (region I) from being drawn towards the core region of the embedding atoms (region II), we apply a boundary condition by introducing an orthogonality constraint term $V_{\rm or}$ in the potential. This is defined as

$$V_{\rm or}=\begin{cases}2\displaystyle\sum_{j=1}^{M_{\rm II}}\frac{Z_j}{|\mathbf{r}-\mathbf{R}_j|} & \text{if } \mathbf{r} \text{ is in the core areas of surrounding atoms}\\ 0 & \text{otherwise.}\end{cases} \quad (6)$$

If $\rho_{\rm I}(\mathbf{r})$ satisfies the condition

$$\rho_{\rm I}(\mathbf{r})|_{r_c}=0 \quad (\text{where } r_c \text{ denotes } r \text{ in the core areas of surrounding atoms}), \quad (7)$$

we have

$$\int \rho_i(\mathbf{r}) V_{\rm or}(\mathbf{r}) d\mathbf{r} = 0. \tag{8}$$

Thus the total energy of the embedded cluster (regions I and II) can be rewritten with the added term in Eq. (8) as

$$E_G[\rho] = T[\rho] + E_{\rm xc}[\rho] + \int\int \frac{\rho(\mathbf{r})\rho(\mathbf{r}')}{|\mathbf{r}-\mathbf{r}'|}\, d\mathbf{r}\, d\mathbf{r}' - 2\sum_{i=1}^{M} \int \frac{\rho(\mathbf{r}) Z_i}{|\mathbf{r}-\mathbf{R}_i|}\, d\mathbf{r} + \sum_{\substack{i,j \\ i\neq j}}^{M} \frac{Z_i Z_j}{|\mathbf{R}_i-\mathbf{R}_j|} + \int \rho_{\rm I}(\mathbf{r}) V_{\rm or}(\mathbf{r}) d\mathbf{r}. \tag{9}$$

The variational solution of Eq. (9) yields the basic formula of the SCCE method.[3–5]

$$\left(-\nabla^2 + 2\int \frac{\rho_{\rm I}(\mathbf{r}') + \rho_{\rm II}(\mathbf{r}')}{|\mathbf{r}-\mathbf{r}'|}\, d\mathbf{r}' - 2\sum_{i=1}^{M} \frac{Z_i}{|\mathbf{r}-\mathbf{R}_i|} + V_{\rm xc}^{\sigma}(\mathbf{r}) + V_{\rm or} \right) \phi_n^{\sigma}(\mathbf{r}) = \lambda_n^{\sigma} \phi_n^{\sigma}(\mathbf{r}). \tag{10}$$

It is important to point out that addition of the orthogonality constraint in Eq. (10) does not affect the total energy. It simply keeps the electrons of region I from collapsing into the atomic core areas of region II.

For the perfect system, the following model is used to solve Eq. (10). (a) The boundary condition for $\phi_n^{\sigma}(r)$ is finite instead of periodic,

$$\phi_n^{\sigma}(r)\big|_{r\to\infty} = 0. \tag{11}$$

(b) The charge and spin densities have the periodicity of the crystal. This is achieved by the self-consistent solution of Eq. (10): $\rho_{\rm II}(\mathbf{r})$ is identical to the periodic extension of $\rho_{\rm I}(\mathbf{r})$,

$$\rho_{\rm II}(\mathbf{r}) = \sum_{\alpha\neq 0} \rho_{\rm I}(\mathbf{r}-\mathbf{R}_\alpha). \tag{12}$$

So the embedded cluster represents a portion of the crystal. This guarantees that the total charge density $\rho(\mathbf{r})$ makes the total energy $E_G[\rho]$ in Eq. (1) minimum, i.e., we obtain the correct periodic charge and spin densities of the crystal.

When the above method is applied to the impurity problem, modifications are necessary. (i) A new cluster containing the impurity at the center and layer of host atoms surrounding it is taken as region I, which is solved exactly. (ii) The impurity-containing cluster is embedded inside the crystal. A cluster, separate from the one considered from the perfect host system, is constructed to simulate the embedding medium. (iii) The charge density $\rho_{\rm II}$ in this medium is taken to be the same as that derived in the perfect host system.

The total ground-state energy of the crystal containing a defect is given as[3]

$$E_{\rm I}[N_{\rm I}, M_{\rm I}] = T[\rho_{\rm I}] + E_{\rm xc\ I}[\rho_{\rm I}, \rho_{\rm II}] + \int\int \frac{\rho_{\rm I}(\mathbf{r})\rho_{\rm I}(\mathbf{r}')}{|\mathbf{r}-\mathbf{r}'|}\, d\mathbf{r}\, d\mathbf{r}' + \int\int \frac{\rho_{\rm I}(\mathbf{r})\rho_{\rm II}(\mathbf{r}')}{|\mathbf{r}-\mathbf{r}'|}\, d\mathbf{r}\, d\mathbf{r}' - 2\sum_{i=1}^{M} \int \frac{\rho_{\rm I}(\mathbf{r}) Z_i}{|\mathbf{r}-\mathbf{R}_i|}\, d\mathbf{r} + \sum_{i=1}^{M_{\rm I}} \sum_{\substack{j=1 \\ j\neq i}}^{M} \frac{Z_i Z_j}{|\mathbf{R}_i-\mathbf{R}_j|}$$

with

$$E_{\rm xc\ I}[\rho_{\rm I}, \rho_{\rm II}] = \int \sum_{\sigma} \rho_{\rm I}^{\sigma} \epsilon_{\rm xc}(\rho^{\uparrow}, \rho^{\downarrow}) d\mathbf{r}. \tag{13}$$

$N_{\rm I}$ is the number of electrons in region I. Since the embedding environment (region II) depends on the geometry of the central cluster containing the defect (region I), it is not possible to compare the energies of the perfect and defected system to calculate, for example, the vacancy formation energy. However, our interests here are to locate the position and energetics of hydrogen atoms inside a vacancy. In this case, the central cluster composition (region I) is fixed. We only allow the hydrogen atoms to change their site inside the vacancies to determine their equilibrium position. Since region II is fixed and we are only interested in the relative energies with respect to the hydrogen site, we do not need to take into account the contributions of region II atoms to the total energy. Thus, for studying the energetics of the impurity, we evaluate the energy difference term ΔE,

$$\Delta E_{\rm I}[\rho_{\rm I}, M_{\rm I}] = T[\rho_{\rm I}] + E_{\rm xc}[\rho] + \int\int \frac{\rho_{\rm I}(\mathbf{r})\rho_{\rm I}(\mathbf{r}')}{|\mathbf{r}-\mathbf{r}'|}\, d\mathbf{r}\, d\mathbf{r}' + 2\int\int \frac{\rho_{\rm I}(\mathbf{r})\rho_{\rm II}(\mathbf{r}')}{|\mathbf{r}-\mathbf{r}'|}\, d\mathbf{r}\, d\mathbf{r}' - 2\sum_{i=1}^{M} \int \frac{\rho_{\rm I}(\mathbf{r}) Z_i}{|\mathbf{r}-\mathbf{R}_i|}\, d\mathbf{r} - 2\sum_{j=1}^{M_{\rm I}} \int \frac{\rho_{\rm II}(\mathbf{r}) Z_j}{|\mathbf{r}-\mathbf{R}_j|}\, d\mathbf{r} + \sum_{\substack{i,j \\ j\neq i}}^{M} \frac{Z_i Z_j}{|\mathbf{R}_i-\mathbf{R}_j|} - \sum_{\substack{i,j \\ j\neq i}}^{M_{\rm II}} \frac{Z_i Z_j}{|\mathbf{R}_i-\mathbf{R}_j|}. \tag{14}$$

The binding energy E_b of n hydrogen atoms in a vacancy is given by

$$E_b = (E_{v+n\rm H} - E_v) - E_{n\rm H} = (\Delta E_{v+n\rm H} - \Delta E_v) - E_{n\rm H}, \tag{15}$$

where $E_{v+n\rm H}$ is the energy of the system containing n hydrogen atoms inside the vacancy. E_v is the corresponding energy without the hydrogen atoms. Note that E_b is independent of whether Eq. (13) or (14) is used.

To solve Eq. (10) and (14), the single-particle wave functions are expanded into a set of Gaussian orbitals.[3,4] The calculation uses all electrons, that is, no pseudopotential or frozen-core approximations are used. Table I gives our basis sets for Ni and H, which are based on those originally provided by Wachters[10] and van Duijneveldt.[11] The nickel $3d$ bases were reoptimized by Rappe, Smedley, and Goddard.[12] For hydrogen, the contraction coefficients were provided by

TABLE I. Basis sets for (a) the Ni atom and (b) the H atom.

(a)

$s(10)$		$p(5)$		$d(7)$	
Exponent	Coefficient	Exponent	Coefficient	Exponent	Coefficient
284 878.0	0.000 32	1774.180	0.002 95	58.730 00	0.175 529 262
4 1997.90	0.002 46	423.4030	0.023 37	16.710 00	0.100 405 05
9627.670	0.012 54	138.3110	0.104 06		
2761.960	0.049 26	53.170 30	0.282 26	5.783 000	1.000 00
920.4880	0.149 50	22.387 40	0.434 86	2.064 000	1.000 00
341.8050	0.326 40			0.771 661	1.000 00
		9.928 430	1.000 00	0.335 505	1.000 00
138.0230	0.404 74	4.116 250	1.000 00	0.156 049	1.000 00
59.258 70	0.191 86	1.710 310	1.000 00	0.080 025	1.000 00
		0.672 528	1.000 00		
20.371 20	1.000 00				
8.594 000	1.000 00				
2.394 170	1.000 00				
0.918 169	1.000 00				
0.202 922	1.000 00				
0.101 461	1.000 00				
0.054 844	1.000 00				
0.032 261	1.000 00				

(b)

		$s(6)$			
Exponent	Coefficient	Exponent	Coefficient	Exponent	Coefficient
402.009 95	0.000 279	1.282 709	1.000 00	0.035 000	1.000 00
60.241 959	0.002 165	0.465 544	1.000 00		
13.732 173	0.011 200	0.181 120	1.000 00		
3.904 505 0	0.044 899	0.072 791	1.000 00		

Lie and Clementi.[13] A few diffuse bases have also been added. The same basis sets were used in all of the following calculations.

III. RESULTS AND DISCUSSION

In the following, we discuss our results on pure Ni, monovacancy in Ni, and vacancy-hydrogen complexes in Ni separately.

A. Electronic structure of Ni

We have calculated the electron charge density, molecular energy-level structure, binding energies, and magnetic moments of pure Ni using the self-consistent cluster-embedding technique for two reasons. (i) A comparison of our results with numerous theoretical results based on band-structure methods and with experiments can allow us to judge the merit of the SCCE method. (ii) In the study of defects in Ni, we need to know the charge-density distribution in the embedding region (region II). Studying the perfect system will provide that information.

The perfect Ni metal was modeled by a six-atom Ni_6 cluster embedded in a sea of 158 Ni atoms. The later atoms simulate region II where the charge density is given by ρ_{II}. Region II corresponds to all atoms confined within a sphere of radius $\sqrt{4.25}a_0$. The center of this sphere lies at the center of the Ni_6 cluster representing region I. The atoms in the Ni_6 cluster are at the fcc sites of a cube with edge length of $a_0=3.523\,87$ Å. This corresponds to the fcc ferromagnetic Ni in bulk.[14]

As shown in Table I(a), each nickel atom has 60 bases. For the Ni_6 cluster, the total number of bases is 360. A total number of 168 bases are used to fit the charge density. A total of 221 788 grid points filling a cube of $3a_0\times3a_0\times3a_0$ and a sphere with radius of $2.07a_0$ (both are centered at the origin) are used for the calculation of V_{xc}. V_{or} is evaluated numerically in each core region of the surrounding atoms. The radius of surrounding atomic core region, r_0, is adjusted according to two simple rules: (i) avoid numerical instability and (ii) keep the total energy minimum. After several trial calculations, we find the optimum value of r_0 to be 0.782 a.u. A total of 1806 grid points are included in each core region. The converged results show that only 0.0013 cluster electrons remain in the 158 surrounding Ni atomic core regions, which means that the condition (7) is well satisfied.

In Fig. 1 we plot the electron eigenvalues for spin up and down. We note that the Fermi energy passes through the highest occupied molecular orbital (HOMO) levels, indicating that the SCCE method yields a metallic ground state. The electronic states at the Fermi energy are composed of a hybrid of $4s$ and $3d$ states. The solid lines represent occupied states, while the dashed lines are for unoccupied states. We see that the $4s$ electrons are at both the top and the bottom of the valence states. The bandwidth of $3d$ electrons is about

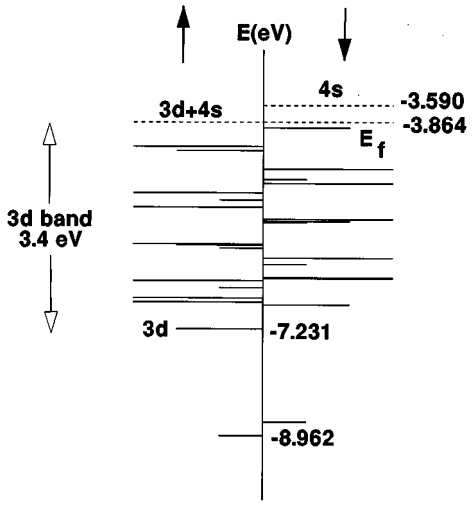

FIG. 1. Electron energy levels of a Ni_6 cluster.

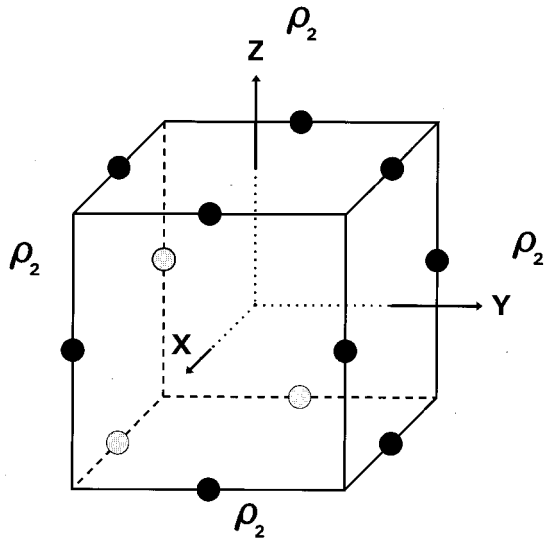

FIG. 2. Geometry of the 12-Ni-atom plus vacancy embedded cluster used to model a vacancy in Ni.

3.4 eV, which agrees with the experimental data of 3.4 eV. The exchange splitting of $3d$ states defined as the energy difference between the eigenvalues of spin up and down states at the HOMO level is 0.38 eV, which agrees well with the experimental result of 0.31 eV. The magnetic moment is calculated to be $0.5\mu_B$/atom and the moments of all six atoms in the Ni_6 cluster are aligned ferromagnetically. This agrees with the experimental data on bulk Ni, where each site has a total magnetic moment of $0.606\mu_B$ with $0.54\mu_B$ coming from the local spin magnetic moment and $0.066\mu_B$ from the orbital angular momentum. The numerical integrals show that in a sphere of radius 4.71 a.u. centered at the nickel atomic nucleus, the total number of electrons is 27.2128. The total energy of the embedded Ni_6 cluster calculated according to Eq. (13) is $-18\,074.7051$ Ry. We have calculated the total energy of a single free Ni atom by using the same basis set to be -3011.9035 Ry. Thus the calculated binding energy per atom in Ni is -0.547 Ry. This needs to be compared with the experimental value of -0.32 Ry.[15] The source of this discrepancy could be due in part to our local-density approximation[16] and the basis-set superposition error.[17] We also note that a small error in the energy of the Ni free atom could contribute significantly to the discrepancy noted above. This, however, would not be a factor in our following discussions of hydrogen trapping energy.

B. Monovacancy in Ni

The cluster used to model a vacancy in Ni is shown in Fig. 2. It contains a vacancy at the center surrounded by 12 Ni atoms. This cluster is then embedded in a host environment that contains 188 atoms. These correspond to all Ni atoms lying within a radius of $\sqrt{5}a_0$ from the vacancy center. The charge density distribution ρ_{II} in the embedded region II is taken as the same charge density derived in Sec. III A. The radius of surrounding Ni atomic core region is unchanged, which is 0.782 a.u. Here we have two basic assumptions. (i) There is no electron charge transfer between the cluster atoms (region I) and the surrounding atoms (region II). (ii) Only the nearest 12 Ni atoms of a vacancy are permitted to change their electron charge density during the variational calculation, while all other nickel atoms are allowed to retain their bulk values. This assumption is imposed by computational limitations.

The bases of Ni atoms are unchanged. In order to avoid the basis-set superposition error,[17] the central vacancy was allotted a set of bases, but no charge. So the total number of bases is 780. A total number of 364 bases are used to fit the charge density. A total of 270 150 grid points, filling a cube of $3a_0\times3a_0\times3a_0$ and a sphere with radius $12a_0/7$ (both are centered at the origin), are used for the calculation of V_{xc}. The converged results show that there are only 0.0016 cluster electrons remaining in the core regions of surrounding 188 nickel atoms, which means that Eq. (7) is again well satisfied.

Figure 3 gives the calculated eigenvalues of the embedded 12 Ni atoms plus vacancy cluster. An important change from the perfect system is that there are no $4s$ electrons at the Fermi energy. But the states at the Fermi energy are still partly filled, which means that the Ni atoms near a vacancy still have metallic property. The Mulliken populations show

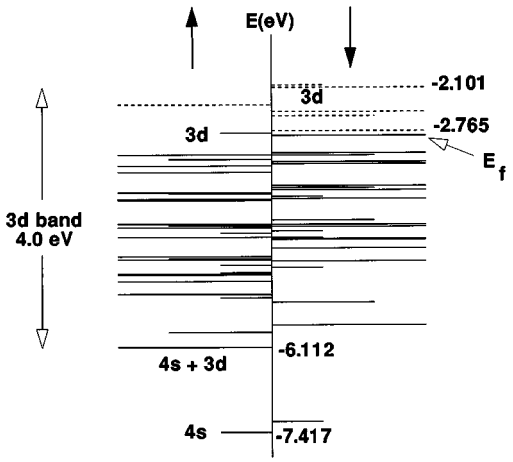

FIG. 3. Electron energy levels of the 12-Ni-atom plus vacancy cluster.

that each nickel atom has a local-spin magnetic moment of $0.67\mu_B$ and the moments are aligned ferromagnetically. This is larger than the bulk value of $0.5\mu_B$ by about 30%. Numerical integration shows that in the central vacancy area (radius 4.71 a.u.), there are 0.526 electrons. In each nickel atom area (radius 4.71 a.u.) the total number of electrons is 27.171, which is a little less than that of the bulk state. This means that some electron charges have moved to the vacancy region.

In order to study the effect of the vacancy on the electronic structure, we compare the eigenvalues in Fig. 3 with those in Fig. 1. Since the two systems have a different number of cluster atoms and surrounding atoms, the absolute energy scales and the density of states are different and we can only compare their relative properties. In general, the two figures are similar, except for the following. (i) The vacancy state has more $4s$ electrons at the bottom of valence band. (ii) The Fermi energy of the vacancy state is in the $3d$ band, while the Fermi energy of the bulk state is between the $3d$ band and the $4s$ band. (iii) The $3d$ bandwidth of the vacancy state is about 4.0 eV and is larger than the value of bulk state, which is 3.4 eV. This difference could be due in part to our choice of two different clusters that model the perfect bulk and the vacancies. However, this will not affect our studies of hydrogen decoration since we use the same cluster environment. In conclusion, we found that the vacancy state in Ni enhanced the local magnetic moment, keeping the spin alignment intact.

C. Vacancy-hydrogen complex

Now we perform the calculations on the vacancy-hydrogen complex. In this section, the solid environment and the grid points used for the calculation of $V_{\rm xc}$ are the same as that for the vacancy calculation in Sec. III B. The basis set for nickel atom is also the same as that in Sec. III B. The only difference is that we add the hydrogen atoms in the vacancy. The basis set of the hydrogen atom is shown in Table I.

First, we calculate a cluster of 12 Ni atoms plus vacancy plus one H atom embedded into a 188-Ni-atom atomic array (region II). The hydrogen atom is at the center of the vacancy. The total number of bases is 726. The charge density was fitted to 345 bases. The converged results show that there are 0.0016 cluster electrons remaining in the core regions of surrounding 188 nickel atoms, which means that the condition in Eq. (7) is well satisfied. Figure 4 shows the eigenvalues and the Mulliken populations of the cluster. We see that there are no s electrons at the top of the valence band. The states at the Fermi energy belong to Ni $3d$ electrons and are partly filled, which means that they still have a metallic property. The cluster still shows the ferromagnetic property, but the local-spin magnetic moment of each nickel atom is reduced to $0.585\mu_B$. The total energy of the cluster containing a single hydrogen at the center of a vacancy is 0.0925 Ry lower than that of an undecorated vacancy. Note that it takes 0.1636 Ry/atom to dissociate a H_2 molecule to individual hydrogen atoms. The above result, therefore, indicates that if vacancy trapping of hydrogen is to be energetically favorable, the equilibrium hydrogen site would be an off-center site. This is in agreement with the result obtained from the effective-medium theory.

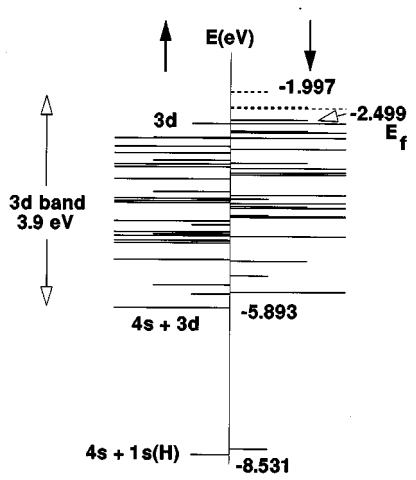

FIG. 4. Electron energy levels of the 12-Ni-atom plus vacancy cluster with a hydrogen atom at the vacancy center.

The calculations of the embedded cluster of 12 Ni atoms plus vacancy plus 6H atoms involves the determination of the positions of the six hydrogen atoms. To determine this, we confined the six hydrogen atoms symmetrically along three coordinate axes. We then varied the distance r of hydrogen from the center of the cluster within the range $r=0.20a_0/2-a_0/2$ (see Fig. 2). The local-spin magnetic moments of the 12 nearest nickel atoms and the binding energy of six hydrogen atoms are given in Fig. 5. We see that as the hydrogen atoms go from the center to the outside, the local-spin magnetic moments decrease. At the position of $0.8a_0/2$, they are almost zero. When the hydrogen atoms reach sites equivalent to the oxygen site in NiO ($r=a_0/2$), the 12 nearest nickel atoms have a small local-spin magnetic moment, but in the opposite direction. This can be seen from the energy-level diagram in Fig. 6. Here we have plotted the spin-up and -down levels for the six hydrogen atoms displaced a distance of $a_0/2$ from the vacancy center. In contrast to the energy-level structures in Figs. 1, 3, and 4, a deep hydrogen $1s$ state appears in Fig. 6. Moreover, the $3d$-band width is reduced to 3.2 eV. The most important feature, however, is that the Fermi energy passes through the spin-up $3d$

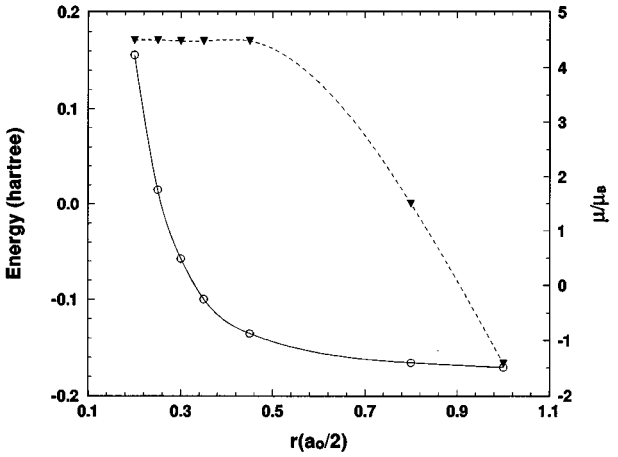

FIG. 5. Variation in the Ni magnetic moment and hydrogen binding energy as a function of distance inside a Ni vacancy.

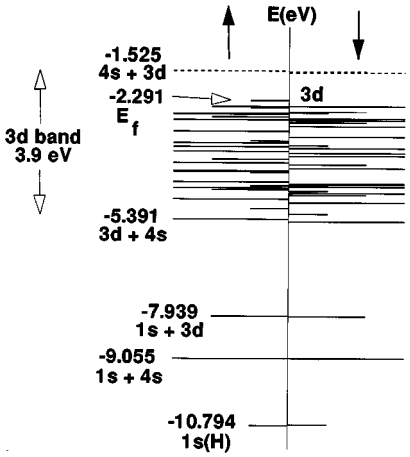

FIG. 6. Electron energy levels of the 12-Ni-atom plus vacancy plus 6-H-atom cluster.

states as opposed to spin-down $3d$ states in the previous case. This means that the magnetic moments at the nearest Ni atoms have flipped their direction and are coupled antiferromagnetically to the surrounding lattice.

From the energetics of the six-hydrogen complex in Fig. 5 we note that the equilibrium position of the six hydrogen atoms in a vacancy is at a distance $r \cong a_0/2$ from the vacancy center. This is similar to the position oxygen atoms occupy in NiO. The energy of the six-hydrogen complex in this configuration is 5.2 eV lower than the bare vacancy plus three isolated hydrogen molecules. It is difficult to assign much quantitative significance to this binding energy for several reasons. (i) Determination of the binding energy using Eq. (15) requires a knowledge of the total energy of the vacancy with and without the decorated-hydrogen atoms. Since the energy differences are very small compared to the total energy of the system, it is important that all the atoms in both systems are treated properly. In our present calculation, the embedding potential arising from region II is taken to be the same for Ni containing either a vacancy or a vacancy-hydrogen complex. Clearly, when a vacancy contains as many as six hydrogen atoms, the host atoms in the embedding region are bound to ''feel'' their presence. It is therefore preferable to recalculate the embedding potential for each situation. We have not attempted these calculations since they are computationally expensive. (ii) The calculation does not take into account the relaxation of the host lattice around the vacancy and the vacancy-hydrogen complex. Again, one expects the relaxation to be different in these cases. (iii) No vibrational contributions to the binding energy of the hydrogen atoms have been included. These contributions are expected to be significant. However, what can be said about our calculations of the energetics is that the preferred site of the hydrogen atoms in the vacancy–6-H-atom complex is similar to that for oxygen in NiO. More importantly, our calculations of the electronic structure and magnetic properties of the vacancy-hydrogen complex are expected to be less sensitive to the above approximations.

Meyers *et al.*[2] have studied the multiple trapping of hydrogen atoms inside a vacancy in Ni by using the effective-medium theory. They have found that the binding energy is 2.1 eV lower than that when the hydrogen atoms occupy the interstitial sites. Since the vacancy formation energy[18] in Ni is 1.5 eV, it implies that vacancy trapping of multiple hydrogen atoms is energetically favorable. It should be pointed out that these authors have ignored the effect of lattice relaxation as well as the vibrational properties of hydrogen in computing the hydrogen binding energy. These calculations therefore provide a qualitative interpretation of Fukai and Okuma's experiment.[1] It should be emphasized that the effective-medium theory cannot provide any information on the effect of multiple hydrogen decoration in vacancies on the electronic structure and magnetic properties.

IV. CONCLUSION

Using a self-consistent cluster-embedding scheme, we have calculated the electronic structure, energetics, and magnetic moments of pure Ni and Ni containing vacancies as well as vacancy-hydrogen complexes. A comparison of our results on the $3d$-band width, the magnetic moment, and cohesive energies in pure Ni with experiment leads us to believe that the SCCE method can be successfully applied to study properties of crystalline materials.

We then used this method to study the binding energies of hydrogen atoms to vacancies and the preferred location inside the vacancies. We found that a single hydrogen atom would not preferentially locate at the center of a vacancy. The equilibrium location of six hydrogen atoms is along the octahedral directions displaced by $a_0/2$ (a_0 being the lattice constant) from the vacancy center. This is similar to the positions of oxygen in NiO. The binding energy of the six hydrogen atoms inside the vacancy exceeds that of the $3H_2$ molecules, confirming the stability of such a complex. In addition, this gain in energy is larger than the vacancy formation energy. Thus hydrogen can induce vacancy formation as suggested by the experiment of Fukai and Okuma and earlier results of Meyers *et al.* based on the effective-medium theory.

The electronic structure of the vacancy-hydrogen complex is also very interesting. As hydrogen atoms move away from the vacancy center, the magnetic moments of the nearest Ni atom continually decrease, and the hydrogen atoms reach their equilibrium configuration, the magnetic moment couples antiferromagnetically to the lattice. This prediction should be verifiable in the hydride phase.

ACKNOWLEDGMENT

This work was supported in part by the Army Research Office (Grant No. DAAL 03-92-G-0106.)

*Present address: Pohl Institute of Solid State Physics, Tongji University, Shanghai 200 092, China.

[1] Yuh Fukai and Nobuynki Okuma, Jpn. J. Appl. Phys. **32**, L1256 (1993).
[2] S. M. Myers, P. Nordlander, F. Besenbacher, and J. K. Norskov, Phys. Rev. B **33**, 854(1986); F. Bessenbacher *et al.*, J. Fusion Energy **9**, 257 (1990).
[3] H. Zheng, Phys. Rev. B **48**, 14 868 (1993).
[4] H. Zheng, Ph.D. thesis, Louisiana State University, 1993 (unpublished).
[5] H. Zheng, Physica B **212**, 125 (1995).
[6] P. Hohenberg and W. Kohn, Phys. Rev. **136**, B864 (1964).
[7] W. Kohn and L. J. Sham, Phys. Rev. **140**, A1133 (1965).
[8] U. von Barth and L. Hedin, J. Phys. C **5**, 1629 (1972).
[9] A. K. Rajagopal, S. Singhal, and J. Kimball (unpublished), as cited by A. K. Raiagopal, in *Advances in Chemical Physics*, edited by G. I. Prigogine and S. A. Rice (Wiley, New York, 1979), Vol. 41, p. 59.
[10] A. J. H. Wachters, J. Chem. Phys. **52**, 1033 (1970).
[11] F. B. van Duijneveldt, IBM Res. Dev. **945**, 16 437 (1971).
[12] A. K. Rappe, T. A. Smedley, and W. A. Goddard III, J. Phys. Chem. **85**, 2607 (1981).
[13] G. L. Lie and E. Clementi, J. Chem. Phys. **60**, 1275 (1974).
[14] R. W. C. Wyckoff, *Crystal Structures* (Interscience, New York, 1965), Vol. 1.
[15] W. P. Mason, *Physical Acoustics* (Academic, New York, 1965); K. A. Gschneider, Jr., Solid State Phys. **16**, 276 (1964); *American Institute of Physics Handbook*, 3rd ed. (McGraw-Hill, New York, 1970); M. Rosen, Phys. Rev. **165**, 351 (1968); G. R. Love, C. C. Koch, H. L. Whaley, and Z. R. Mcnutt, J. Less Common Metals **20**, 73 (1970); S. B. Palmer and E. W. Lee, Philos. Mag. **24**, 311 (1971); J. A. Rayne and B. S. Chandrasekhar, Phys. Rev. **122**, 1714 (1961); E. S. Fisher and D. Dever, Trans. Metall. Soc. AIME **239**, 48 (1967); G. A. Alers, J. R. Neighbours, and H. Sato, J. Phys. Chem. Solids **13**, 40 (1960).
[16] V. L. Moruzzi, J. F. Janak, and A. R. Williams, *Calculated Electronic Properties of Metals* (Pergamon, New York, 1978).
[17] S. F. Boys and F. Bernardi, Mol. Phys. **19**, 553 (1970).
[18] H. J. Wollenberger, *Physical Metallurgy*, edited by R. W. Cahn and P. Haasen (Elsevier, Amsterdam, 1983), p. 860.